Where photons meet phonons
Buters, F.M.

Author: Buters, F.M.
Title: Where photons meet phonons
Issue Date: 2017-12-21

11

Outlook: High-Q membranes, Coherent state transfer and Future directions

In the previous chapter we learned that optical absorption is one of the limiting factors in reaching the quantum mechanical ground-state. If the mechanical Q-factor of the trampoline resonator would be significantly higher, ultra low cryogenic temperatures are no longer needed which reduces the impact of optical absorption. Both issues, moderate Q-factor and optical absorption, can be addressed by replacing the trampoline resonator with a thin silicon nitride membrane. In this chapter we will give a brief introduction to silicon nitride membranes and compare them to our current trampoline resonators.

Apart from the issue of optical absorption, the optomechanical experiment in a cryogen free dilution refrigerator functioned as expected. It is therefore time to look at the generation of the superposition state needed to investigate gravitationally induced decoherence. The original idea proposed by Marshall [8] uses an optical cavity with a movable end mirror, just like our set-up. The optomechanical cavity is then combined with an additional cavity to form a Michelson interferometer to create entanglement between the path of the photon and the state of the mechanical resonator. In order to be able to measure any novel decoherence at all, the optomechanical coupling rate needs to be larger than the mechanical frequency. This requirement turns out not to be feasible. One solution would be to use a second mechanical resonator instead of an additional optical cavity. Via coherent optomechanical state transfer a superposition state between two mechanical resonators can be created. This idea, proposed by Matthew Weaver, is already explored experimentally in the classical domain, and some of the results will be discussed in this chapter.

Finally, we will briefly which optomechanical platform is the best to investigate the coherent state transfer. We take a closer look at photonic crystal nanobeam cavities. Because the mechanical frequency of the nanobeam can be in the GHz range,

---

Part of the work presented in this chapter is based on: M.J. Weaver, F.M. Buters, J. Luna, H. Eerkens, K. Heeck, S. de Man and D. Bouwmeester, "Coherent optomechanical state transfer between dissimilar mechanical modes", accepted for publication in Nature Communications (see arXiv:1704.02394) cryogenic cooling suffices to prepare the system in the quantum mechanical ground-state. Combined with relatively high single-photon coupling rates, these systems are well suited to perform quantum experiments with mechanical resonators.

11.1 High-Q silicon nitride membranes

The current sample design, a trampoline resonator with a DBR mirror, has the advantage of the high quality mirror. This results in a high finesse optical cavity as is demonstrated in chapter 5. The downside however, is that the same DBR mirror introduces significant losses for the mechanical motion of the trampoline resonator. This has been investigated by M. Weaver and F. Luna at UCSB by comparing trampoline resonators with and without DBR mirror. Although the frequency increases by a factor of two for the resonator without mirror, the mechanical quality factor is also consistently higher by at least a factor of two. So far no progress has been made in reducing the mechanical losses introduced by the DBR mirror.

In addition to the cavity geometry used in this work, namely a cavity with a movable end mirror, a different geometry can also be used in which a silicon nitride membrane is placed in between two high quality mirrors. This membrane-in-the-middle approach has several advantages. For example, the coupling of the mechanical motion to the cavity field now depends on the position of the membrane with respect to a node or an anti-node of the cavity field. Positioning the membrane close to an anti-node results in a coupling that scales with the displacement squared [136]. Since the phonon number is directly proportional to the energy of the mechanical mode, which scales as x^2, quantum non-demolition measurements [137] of the phonon number are directly possible [138], without the need for any back-action evading schemes [139]. Also, heating due to optical absorption, a big issue with the current trampoline resonators, can be minimized by placing the membrane at a node.

The most interesting aspect of these membrane-in-the-middle experiments, are the mechanical properties of the membrane itself. The mechanical frequency of these membranes is comparable to our trampoline resonators and also the mode-mass is similar. The mechanical quality factor, however, is much larger. Furthermore, these membranes are commercially available via Norcada Inc. As a demonstration of these high Q-factors, the mechanical properties of several modes of a 2×2 mm, 50 nm thick membrane (Norcada NX5200AS) are measured. The mechanical motion is monitored via a fiber interferometer , while the dielectric force is used for the excitation (see chapter 9). The experiment was conducted at a pressure of 1×10^{-5} mbar.

Figure 11.1(a) shows the mechanical ringdown of a higher order membrane mode, while in (b) the Q-factors for the fundamental and other higher order modes are shown. The Q-factor for the membrane modes is typically ten times higher than the Q-factor of our trampoline resonators. Furthermore, by optimizing the clamping of such a membrane, Q-factors as high as 50×10^6 at room temperature have been achieved using commercially available membranes [140]. Finally, several groups have fabricated custom membranes [141, 142] with Q-factors exceeding 100×10^6. The current record is set by patterning a silicon nitride membrane with a phononic

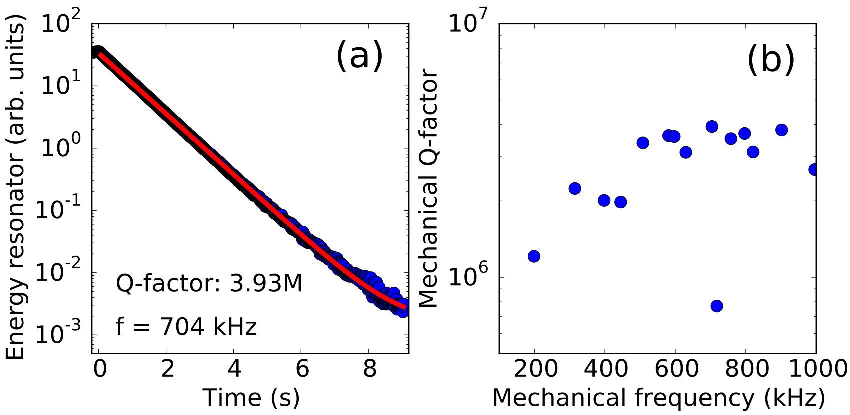

Figure 11.1: Mechanical quality factor of a commercially available silicon nitride membrane. (a) Mechanical ringdown of the (4,3) mode. (b) Mechanical quality factor for the fundamental and higher order modes.

crystal structure. A Q-factor of 214×10^6 is achieved at room temperature for a 777 kHz resonator with a mode-mass of 16 ng [143].

It is not difficult to see why a high-Q membrane will help in reaching the quantum mechanical ground-state. In the previous chapter, we achieved an effective mode temperature of 3.6 mK with optical cooling from a base temperature of 6 Kelvin. Suppose we keep all the parameters the same, including the sample design, and increase the Q-factor from 450×10^3 to 200×10^6. The effective mode temperature will decrease from 3.6 mK to 8.1 μK, which is cold enough for the resonator to be in the ground-state.

We can take this one step further. Suppose that we have placed a high-Q membrane at a node and therefore have reduced the optical absorption. Instead of a base temperature of 6 Kelvin, the temperature is lowered further. Typically the Q-factor increases when the temperature is lowered below 6 Kelvin [144]. As we have seen in chapter 10, the thermal conductivity of silicon nitride decreases significantly when the temperature is lowered below 6 Kelvin. This poses an interesting trade-off. The increase in Q-factor can directly be offset by the decrease in thermal conductivity even when heating due to optical absorption is negligible at 6 Kelvin.

Thermalization and optical absorption of membranes at mK temperatures has not been investigated extensively. Cryogenic and optical cooling have successfully been used by the Harris group to cool a commercial membrane to the quantum mechanical ground-state [97]. This involved a cryostat with a base temperature of 0.8 Kelvin and a commercial membrane with a Q-factor of 10×10^6. It is, however, not beneficial for many other membrane experiments to perform measurements at temperatures below 1 Kelvin. For example, the experiment by the Harris group can also be conducted at 5 Kelvin, if the Q-factor is increased to 63 $\times10^6$.

To summarize, because silicon nitride membranes can have such high Q-factors, dilution refrigerators are no longer required to reach the quantum mechanical ground-

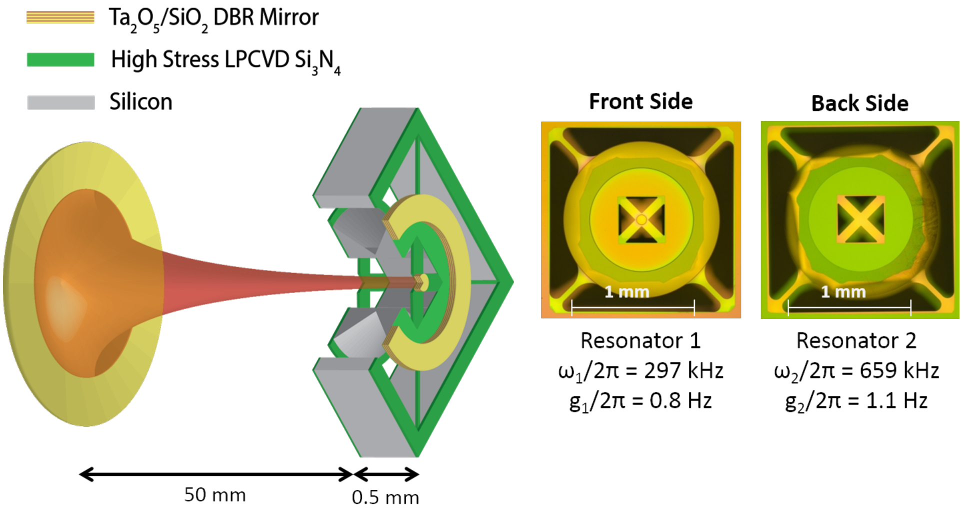

Figure 11.2: Schematic overview of the sample used to demonstrate optomechanical state transfer. The nested resonator design is modified to include a silicon nitride trampoline membrane on the back of the chip. The chip is then oriented such that the membrane sits in the middle of the cavity, and the trampoline resonator with DBR mirror acts as the end mirror of the cavity.

state. A base temperature of 6 Kelvin will suffice, which is beneficial for the heat conductivity of silicon nitride. Finally, optical absorption can be significantly reduced by placing the membrane at a node of the cavity field.

11.2 Coherent optomechanical state transfer

Let us first briefly discuss the idea of generating a superposition state with two mechanical resonators. Suppose two different mechanical resonators are both coupled to the same cavity mode. Furthermore, the two mechanical resonators are both in the quantum mechanical ground state. Via a weak coherent pulse, one resonator is excited to the first excited state. Because both resonators couple to the same optical field, it is possible to swap the excitation of one resonator to the other. If this transfer is done with a $\pi/2$ pulse, a superposition state between the resonators is created. The system can now be set to evolve for some time, after which another $\pi/2$ pulse can be used to bring back the excitation to the first resonator. Finally, a read-out pulse can be used to see if any decoherence has occurred.

The scheme described above requires two mechanical resonators coupled to the same cavity mode and the ability to optically couple the two mechanical resonators. Figure 11.2 shows a realization of two mechanical resonators coupled to the same cavity mode. The design of the nested resonator is expanded to include a silicon nitride trampoline membrane at the back of the chip. A membrane-in-the-middle cavity is created by adding this trampoline membrane. We have verified this ex-

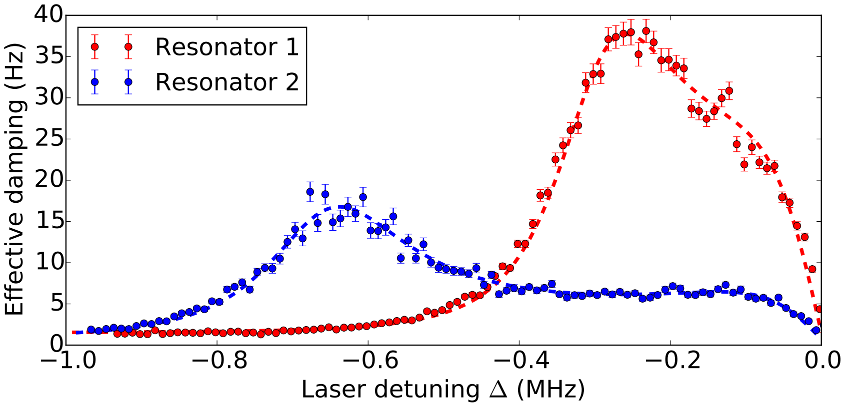

Figure 11.3: Effective damping as a function of laser detuning for a single laser drive. The optomechanical interaction of each resonator is well described by the theory presented in chapter 2.

perimentally by measuring the cavity finesse as function of wavelength, thereby changing the location of the nodes of the cavity field with respect to the trampoline membrane [138].

By measuring simultaneously the effective mechanical linewidth as a function of laser detuning for a single laser drive, see Fig. 11.3, we see that the interaction of each resonator with the optical field can be described by the theory presented in chapter 2. We also obtain an optical linewidth of 200 kHz and the optomechanical coupling g_0 for both mechanical resonators.

Although the resonators are located on the same chip, as is shown in Fig. 11.2, their frequency difference is sufficiently large for them to be mechanically decoupled. The coupling, therefore, is purely optical. Buchmann and Kurn have proposed a method to do this using two laser tones [145], of which the key points will be presented here. Figure 11.4(a) shows schematically the energy diagram for two harmonic oscillators. By choosing the laser frequencies carefully, laser 2 (ω_{L2}) can end up in a mode with the same freqency as laser 1 (ω_{L1}) after interacting with both mechanical resonators. In doing so, a phonon is exchanged from resonator 1 to resonator 2. The requirement for the laser frequencies, $\omega_{L2} + \omega_1 = \omega_{L1} + \omega_2$ can be rewritten as $\omega_{L2} - \omega_{L1} = \omega_2 - \omega_1$, which shows that the two laser tones should be separated by the difference of the mechanical frequencies. In Fig. 11.4(b) the two laser tones are shown together with the optical side-bands generated after interacting with both mechanical resonators. Two pairs of side-bands match up, precisely at the resonance condition for coherent state transfer.

Besides the state transfer, the two tones also generate the "normal" optomechanical effects, such as optical damping. To minimize these effects, both lasers are placed relatively far away from the cavity resonance at a detuning of $\Delta = (\omega_{L1} + \omega_{L2})/2 = -2.3$ MHz. These two tones are generated via an AOM using carrier suppressed side-band generation (see chapter 3). The mechanical motion of each resonator is

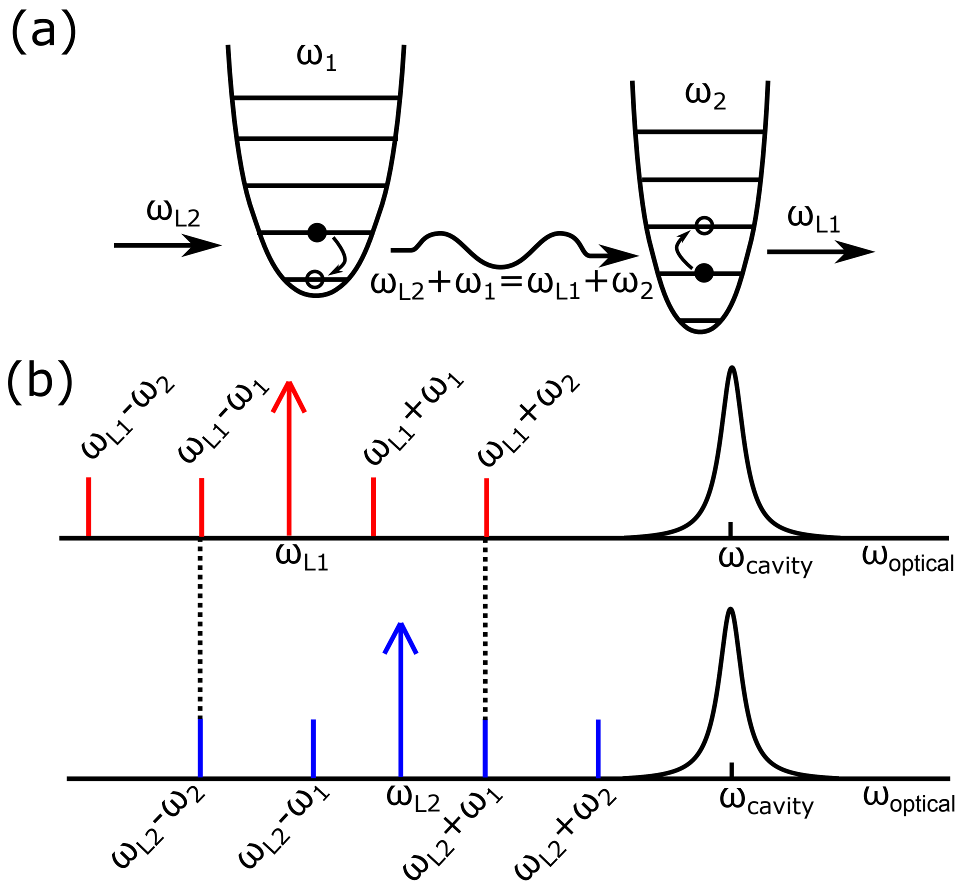

Figure 11.4: (a) Optomechanical state transfer using two laser tones occurs when the difference between the two laser frequencies is precisely the difference between the mechanical frequencies. (b) Schematic overview of the two laser tones together with optical side-bands generated after interacting with both mechanical resonators. Two pairs of side-bands match up, precisely at the resonance condition for coherent state transfer.

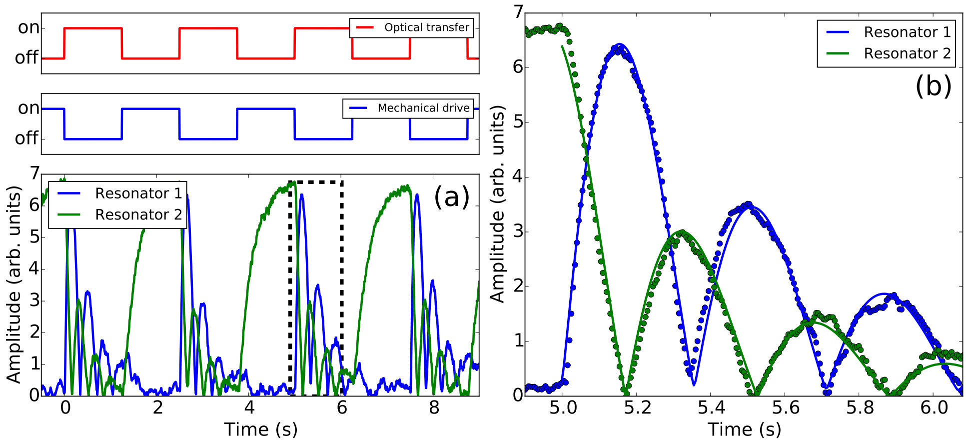

Figure 11.5: (a) Demonstration of optomechanical state transfer. The trampoline membrane, resonator 2, is driven via the dielectric force, after which the two tone laser drive periodically transfers the excitation back and forth between the two resonators. (b) Zoom of the outlined region in (a) showing that the coherent state transfer is well described by two coupled damped harmonic oscillators.

monitored via a probe beam locked with the Pound-Drever-Hall method (PDH) to a cavity resonance. The PDH error is used for feedback as well as for the read-out of the mechanical motion. Using a lock-in amplifier, the error signal is filtered in the frequency domain around the mechanical frequencies of the two resonators. In this way, the amplitude of mechanical motion is obtained.

A difference in energy between the two mechanical resonators is needed for any state transfer to take place. We achieve this by using actuation via the dielectric force, as demonstrated in chapter 9, to drive the trampoline membrane. The results are shown in Fig. 11.5. With the mechanical drive, the amplitude of resonator 2 is increased with respect to thermal motion. When the mechanical drive is turned off and the two lasers are turned on, optomechanical state transfer occurs and energy is periodically transferred between the two mechanical resonators. Figure 11.5(a) displays multiple of these cycles, showing that the transfer is very reproducible. With the two lasers turned on, the optomechanical system is well described by two coupled damped harmonic oscillators, as is shown in Fig. 11.5(b). Furthermore, the amplitude of motion of each resonator periodically drops back to the value corresponding to thermal motion, indicating full state transfer.

The measurements presented so far are a classical demonstration, but from Fig. 11.5 it is clear that an optical pulse of the correct length should be able to partially transfer energy from one resonator to the other, showing that a $\pi/2$ pulse is feasible. The next step is therefore to repeat these experiments at, or close to, the quantum mechanical ground-state together with a rigorous treatment of the quantum mechanical theory of state transfer. For example, both resonators should be cooled to the quantum mechanical ground state after which the state of both resonators can be entangled. As pointed out by Ludwig et al., this is theoretically already a non-trivial problem [146].

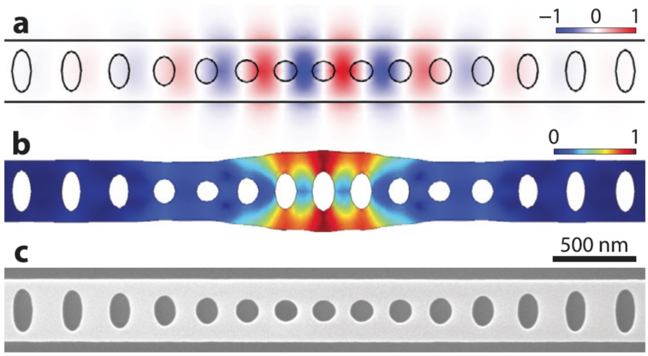

Figure 11.6: Photonic crystal nanobeam cavity in which the optical mode shown in (a) is co-localized with the mechanical mode shown in (b). The whole structure is only a couple of micrometers in size as is shown in the SEM image in (c). This figure is taken from Ref. [118].

11.3 The optimal platform to investigate optomechanical state transfer

The difficulties of ground-state cooling can be reduced by choosing a system with relatively high mechanical frequency, such that the mechanical ground-state can be reached by cryogenic cooling without additional optical cooling. This typically requires a $\sim$ GHz mechanical frequency and mK temperatures. Of the few systems that operate in this regime, photonic crystal nanobeams cavities are a promising candidate for future experiments.

Figure 11.6 shows an example of a photonic crystal nanobeam cavity, as fabricated by the Painter group [118]. The optical mode spatially overlaps with the mechanical mode, creating strong optomechanical coupling. The whole structure is only a couple of micrometers in size. Due to the small mode volume of the cavity and the small mass of the resonator, the optomechanical coupling is quite strong. Furthermore, by decreasing the frequency from $\sim$ GHz to $\sim$ MHz frequencies, record high coupling rates were recently achieved [147].

We can make the comparison between different systems more quantitative by selecting the proper figure of merit. In chapter 4 the optomechanical cooperativity was introduced as $C = C_0 n_{cav}$ where n_{cav} is the cavity photon number and $C_0 = 4g_0^2/\kappa\Gamma_m$ is the single-photon cooperativity. Also the effect of side-band cooling can be expressed in terms of C. When the cooling laser is located at $\Delta = -\Omega_m$ the optical damping rate is given by $\Gamma_{opt} = \Gamma_m C$. As a reference, the system presented in this thesis has $C_0 = 0.003$.

In the quantum regime, the coherent state transfer discussed in the previous section requires single photons to excite one resonator from the ground state to the first excited state. This in turn requires a large single photon cooperativity to have a reasonable success rate. Photonic crystal nanobeam cavities with $\sim$ GHz frequency resonators can have $C_0 = 3$ [148], while a modified design with $\sim$ MHz frequency resonators have achieved $C_0 = 1.1 \times 10^3$ [147]. The trade-off, however, is that these lower frequency resonators are not easily cooled to the ground state, even when cryogenic cooling is combined with optical cooling.

The potential of an optomechanical system which is cooled to the ground state by cryogenic means only, has recently been demonstrated [90]. By placing a photonic crystal cavity in a dilution refrigerator at a base temperature of 25 mK, the mechanical mode at 5.3 GHz was cooled to an average phonon occupation number of 0.025. Via a sequence of optical pulses, non-classical correlations between single photons and phonons have been observed.

These experiments involved a single cavity coupled to a single mechanical mode. Already photonic crystal cavities are fabricated in which a single mechanical resonator couples to two cavities [149], creating the equivalent of a membrane-in-the-middle system. A design for two mechanical resonators coupled to a single optical cavity is recently proposed to create an optomechanically induced effect analogous to a phononic band gap [150]. Furthermore, this design can also be used to investigate the optomechanical state transfer in the quantum regime.

Although the mode-mass of the nanobeam resonators might be too small for observing gravitationally induced decoherence, it would still be interesting to perform other quantum experiments such as an optomechanical Bell test [151] or observing phonon jumps [138]. Alternatively, because of the small size, a network of optomechanical cavities on a single chip can be created, which can lead to interesting many-body effects [152]. Finally, hybrid quantum networks can be constructed by coupling qubits such as quantum dots or NV centers to photonic crystal cavities [153].